

Effect of Heat Treatment Temperature on the Wettability Transition from Hydrophilic to Superhydrophobic on Laser-Ablated Metallic Surfaces

Chi-Vinh Ngo and Doo-Man Chun*

Superhydrophobic metallic surfaces made via pulsed laser ablation have been utilized recently. Immediately after laser ablation, metallic surfaces become hydrophilic. By aging the laser-ablated surface in ambient air for a relatively long period of time (several weeks to several months) or using a chemical coating post process, this type of surface becomes superhydrophobic. Herein, a facile post-process heat treatment that does not use any harsh chemicals is introduced to reduce the wettability transition time from hydrophilicity to superhydrophobicity compared to surfaces treated for extended periods of time in ambient air. Grid patterns are ablated on aluminum, copper, and titanium by a nanosecond pulsed laser. Then, facile post-process heat treatment is applied at different temperatures. The effect of temperature on the wettability transition time is studied. The transition time is reduced from several weeks/months to a few hours. The wettability transition mechanism for each metal is also explained. Additionally, several potential applications, such as self-cleaning, water positioning, and water transport, are proposed.

1. Introduction

Generally, the wettability of a solid surface can be defined by its water droplet contact angle (WDCA). A surface with a WDCA less than 90° is normally referred to as being hydrophilic; alternatively, a surface with a WDCA greater than 90° is hydrophobic. Recently, superhydrophobic surfaces with a WDCA greater than 150° have attracted increased attention due to their potential industrial and biomedical applications. Superhydrophobic surfaces are commonly divided into two classes:

low adhesion to water (i.e., the “lotus effect”) with a low sliding angle (SA) that is typically smaller than 10° and high adhesion to water (i.e., the “petal effect” or “pinning effect”) with a high SA (or even no SA). It is well known that the wettability of a surface is governed by its surface roughness and surface chemical composition. Thus, imparting roughness onto the surface of hydrophobic materials^[1–7] or modifying a rough surface with low-surface energy materials^[8–12] are good ways to fabricate superhydrophobic surfaces.

Superhydrophobic metallic surfaces have been demonstrated in various applications such as self-cleaning,^[13] drag reduction,^[14] anti-icing,^[15] anti-corrosion,^[16] water storage,^[17] and water transport.^[18] A pulsed laser ablation technique has been successfully developed over the past few years to produce superhydrophobic metallic surfaces. Metal surfaces become hydrophilic after laser ablation. By aging the laser-ablated surfaces in


ambient air for a relatively long period of time, the hydrophilic metal becomes hydrophobic or superhydrophobic. Each laser-ablated metal with specific processing parameters requires a different wettability transition time to change from hydrophilic to superhydrophobic. Copper or brass that have been ablated by a nanosecond laser require a transition time of 11–14 days,^[19,20] while aluminum ablated by nanosecond or picosecond lasers requires around 30–40 days.^[21] Additionally, nanosecond-laser-ablated titanium requires around 30 days.^[22] Another approach that can be used to avoid these long aging times in ambient air is to use additional chemical coating post processes such as chemical vapor deposition (CVD),^[23] silanization,^[24] chemisorption,^[25] and dip-coating.^[26] However, these approaches utilize toxic chemicals, and the additional processing sometimes requires more than one day.

To shorten the wettability transition time required to obtain a superhydrophobic surface without using any chemicals, we previously introduced a facile post-process heat treatment after pulsed laser ablation.^[27,28] However, in these studies, we only used a treatment temperature of 100°C . The effect of different heat treatment temperatures on the wettability transition time has yet to be studied. Moreover, we found that the wettability transition mechanism for each metal (copper and stainless steel) was completely different when applying the post-process heat treatment. The mechanism of stainless steel was explained clearly by CO_2 decomposition with a change in the chemical composition, as was measured by energy-dispersive X-ray

Dr. D.-M. Chun, Dr. C.-V. Ngo
School of Mechanical Engineering
University of Ulsan
Ulsan, South Korea
E-mail: dmchun@ulsan.ac.kr

Dr. C.-V. Ngo
Changchun Institute of Optics
Fine Mechanics and Physics
Chinese Academy of Sciences
Changchun, China

The Institute of Optics
University of Rochester
Rochester, New York, USA

 The ORCID identification number(s) for the author(s) of this article can be found under <https://doi.org/10.1002/adem.201701086>.

DOI: 10.1002/adem.201701086

spectroscopy (EDS), as well as with the appearance of a new Fe_3C peak after heat treatment, as was measured by X-ray diffraction (XRD). Alternatively, the mechanism of copper was explained by reduction, with the only change in the chemical composition, as was measured by EDS.

In this research, a nanosecond pulse laser was used to make grid patterns on copper (Cu), aluminum (Al), and titanium (Ti). Metals, including Cu, Al, Ti, and others, are commonly used engineering materials in industry and in daily life because of their mechanical, electrical, and thermal properties. Additionally, pure metals easily show the wettability transition mechanism. Picosecond and femtosecond pulse lasers have commonly been used in research but for industrial applications; nanosecond pulse lasers are particularly desirable due to their cost-effective and fast processing times. Additionally, one of the typical disadvantages of nanosecond pulse lasers, that is, the relatively large burr formation after laser ablation, is utilized effectively in this research. These large burrs act as microstructures that can support water droplets; therefore, the contact area between the metal surface and the water droplet is minimized. After nanosecond pulse laser ablation, these metals were treated at different temperatures. The effect of heat treatment temperature on the wettability transition time was studied. These results could provide a useful guide for selecting suitable treatment temperature and treatment time for other researchers who would like to apply this technique in industrial applications. By using this facile post-process heat treatment after laser ablation, the wettability transition time can be reduced from several weeks or several months to a few hours. Moreover, the mechanisms of the wettability transitions for aluminum and titanium were discussed. These mechanisms were also different from those observed for pure copper and stainless steel (as reported in our previous research).^[27,28] Additionally, the mechanism of copper was confirmed via additional surface analysis, compared with previously reported results.^[27] Furthermore, the superhydrophobicity of laser-ablated Al, Cu, and Ti surfaces was demonstrated to be useful for a variety of potential applications including self-cleaning, water positioning, and water transport.

2. Experimental Section

2.1. Fabrication Process

Experiments were performed on commercial aluminum sheets (Al 99.999%, The Nilaco Corporation, Japan), copper sheets (Cu 99.99 + %, Goodfellow Cambridge Ltd., England), and titanium sheets (Ti 99.5%, The Nilaco Corporation, Japan) that were 0.5 mm thick. A Q-switched Nd:YAG 355 nm UV nanosecond pulsed laser system was used to ablate the metallic surfaces, as shown in Figure 1. The laser source provides a laser beam, which is guided by mirrors. The attenuator controls the intensity of the laser power, and the beam expander increases the diameter of the laser beam. A focusing lens with a 5 μm focal spot diameter converges the laser beam for fabrication. A grid pattern is used here because it is easy and fast to fabricate.

Figure 2 illustrates the resultant superhydrophobic metallic surfaces. Metallic sheets (Al, Cu, and Ti) were first ablated by the laser ablation system with a fabrication area of $5 \times 5 \text{ mm}^2$. The laser ablation parameters were shown as in Table 1, and five samples with a step size of 200 μm were produced for reproducibility. The step size

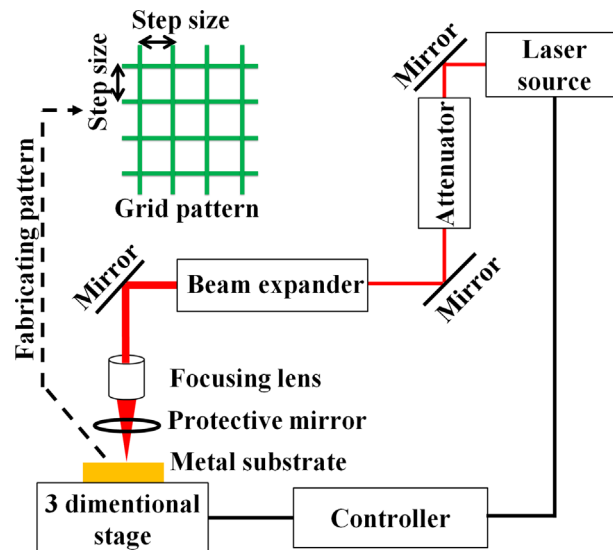


Figure 1. Schematic image of the laser beam texturing system.

or pitch is the distance between laser ablating lines. The laser-ablated surfaces were then placed in a conventional commercial oven at different heat treatment temperatures (100, 150, and 200 °C). The wettability transition was investigated during a treatment time of 24 h. Moreover, additional laser-ablated samples were put in the oven at 50 °C and additional ones were stored in ambient air for a long period of time; these were compared with the samples treated at 100, 150, and 200 °C.

2.2. Surface Characteristics

Field emission scanning electron microscopy (FESEM, JSM-6500F, Jeol Co., Japan) and 3D laser scanning confocal microscopy (VK-X200 series, Keyence, Japan) were used to analyze the surface structures. To evaluate the chemical composition on the surface, X-ray diffraction (ULTIMA IV, Rigaku, Japan), point energy-dispersive X-ray spectroscopy (JSM-6500F, Jeol Co., Japan), and Fourier transform infrared (FT-IR, Varian 670-IR, Varian Inc., USA) spectroscopy at ATR mode (Ge crystal) were carried out. The wettability (contact angle and sliding angle with a 10 μL water droplet) was measured by a contact angle meter (SmartDrop, Femtofab Co. Ltd., Korea).

3. Results

3.1. Surface Morphology

Relatively large burrs around the ablated lines were observed on Al, Cu, and Ti, as shown in Figure 3. Cu showed a wider laser-ablated line between the two lines of burrs than the other metals. The average burr height of laser-ablated Ti was found to be approximately $27 \pm 1.3 \mu\text{m}$, as shown in Figure 4. While Ti showed large burrs with small deviation, Al and Cu showed relatively small burrs (19 ± 2.8 and $19 \pm 1.5 \mu\text{m}$, respectively). In addition, the average aspect ratios (of 10 measurements) between the burr height and the width from the peak to the

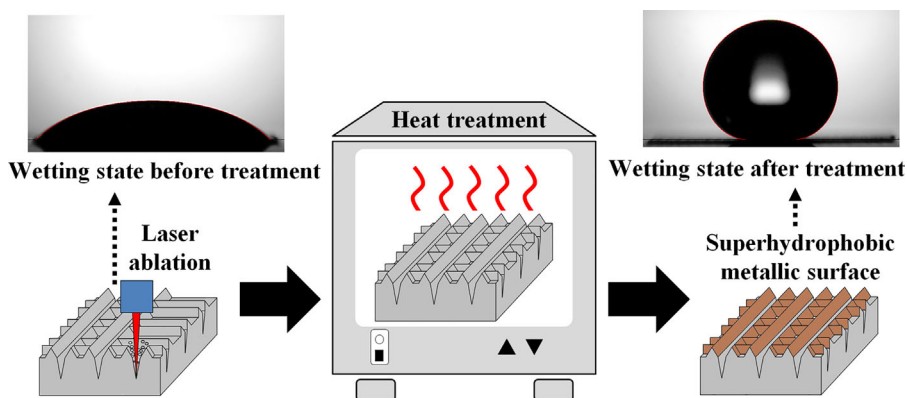


Figure 2. Fabrication process used to make superhydrophobic metallic surfaces.

outside of the burr of Al, Cu, and Ti were 2 ± 0.4 , 3 ± 0.6 , and 5 ± 1.0 , respectively. Among these samples, Ti showed a micro-burr structure with the stiffest outside slope. The measured 3D images were similar to the enlarged and tilted FESEM images. It is usually desirable to minimize burr formation after laser ablation; however, in the present research, larger micro-burrs were useful for improving wettability. For hydrophobic materials, contact angles are larger on microstructures than they are on smooth surfaces. Moreover, the average burr heights of the laser-ablated samples before and after heat treatment were approximately the same.

3.2. Effect of Heat Treatment Temperature on the Wettability Transition

Just after laser ablation, Al, Cu, and Ti showed hydrophilic property. However, after heat treatment in the oven, all samples had increased contact angle values, as shown in **Figure 5**. The error bar indicates the maximum and minimum contact angles/sliding angles for five different samples. The effects of different heat treatment temperatures on the wettability transition time from hydrophilic to superhydrophobic were pointed out. With Al and Ti, as the heat treatment temperature increased, the wettability transition time decreased. Alternatively, for Cu, the wettability transition time was only reduced when the temperature was increased from 100 to 150 °C; at a higher temperature (200 °C), Cu showed a longer wettability transition time compared to that observed at 150 °C. Among the heat treatment temperatures used in this study, Al and Ti showed fast wettability

transition times (90 and 30 min, respectively) at 200 °C, while Cu showed a fast wettability transition (120 min) at 150 °C. After achieving the contact angles greater than 150°, Al, Cu, and Ti surfaces showed superhydrophobic property with high adhesion to water (petal effect). When adding more the heat treatment time, these superhydrophobic surfaces changed from petal effect to lotus effect by appearance of low sliding angles ($SA < 10^\circ$) with a tilting speed of 1.6° s^{-1} . With the exception of Cu, when the heat treatment temperature increased, the sliding angle appeared after a shorter heat treatment time and became smaller gradually with increment of heat treatment time; additionally, the time required to change from petal effect to lotus effect on each metal was different. For example, the sliding angle for Al appeared after 6 h with a heat treatment of 200 °C and after 12 h with a heat treatment of 150 °C. For Ti, the sliding angle appeared after 2 h with a heat treatment of 200 °C and after 12 h with a heat treatment of 150 °C. For Cu, the sliding angle appeared after 12 h with a heat treatment of 150 and 200 °C, and the value for the sample treated at 150 °C was smaller. With increasing treatment time, the sliding angle value for each material decreased. The appearance of the sliding angle and the decrease in the value of the sliding angle might indicate a high-quality superhydrophobic surface that demonstrates the lotus effect. All Al and Cu samples treated at 100 °C failed to show sliding angles within 24 h, even if the samples had a contact angle greater than 150°. Based on the results of Al, Cu, and Ti samples treated at 150 and 200 °C and Ti samples treated at 100 °C, heat treatment time should be increased in order to change the superhydrophobic surface from petal effect to lotus effect on Al and Cu samples treated at 100 °C. Moreover, the Cu samples treated at 200 °C with longer heat treatment times showed reduced superhydrophobicity (i.e., a decrease in CA and an increase in SA).

As the description above, **Figure 5** can provide useful guideline to other researchers and engineers for manufacturing of superhydrophobic surface and the related industry. Depending on the specific requirements, the laser-ablated hydrophilic metallic samples can become superhydrophobic by choosing proper heat treatment temperature and time. For example, to fabricate superhydrophobic Ti for self-cleaning applications and short time fabrication, we can choose 200 °C and 2 h for heat treatment. At that time, contact angle is approximately 170° and

Table 1. Process parameters of laser ablation.

Name of parameter	Value
Power (W)	3
Pulse frequency (kHz)	20
Pulse duration (ns)	20
Laser scan repetition	2
Scanning speed (mm s^{-1})	1

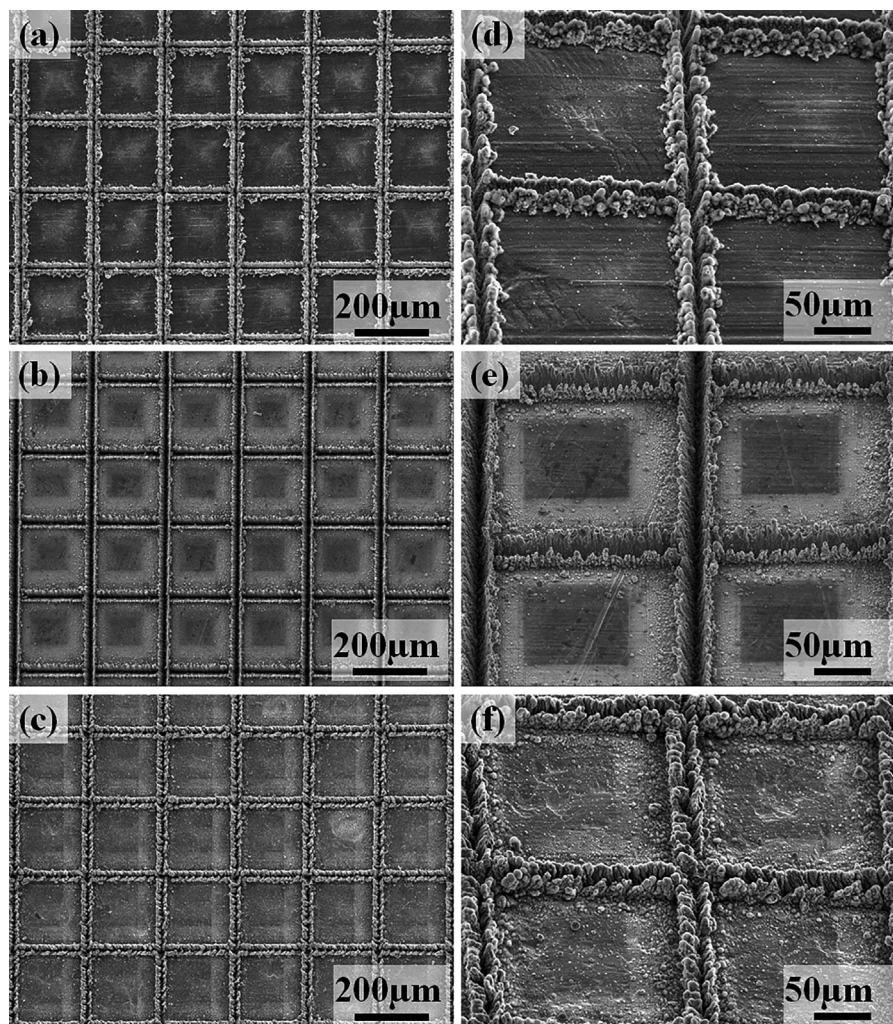


Figure 3. a–c) Top-view FESEM images and d–f) enlarged and tilted images of laser-ablated Al, Cu, and Ti surfaces, respectively.

sliding angle is approximately 10° . But, to fabricate superhydrophobic Ti for high-adhesion applications, short time fabrication, and not high temperature such as 200°C , we can choose 150°C and 6 h for heat treatment. At that time, contact angle is approximately 159° and there is no sliding angle. With Al and Ti, during the heat treatment (a period of 24 h), the contact angle increased from hydrophilic to superhydrophobic and then became stable. Additionally, the sliding angle appeared after a few hours of treatment and then became smaller as a function of time (i.e., better superhydrophobicity). However, with Cu, during the heat treatment (a period of 24 h), the contact angle increased from hydrophilic to superhydrophobic before becoming stable but then started decreasing; additionally, the sliding angle appeared after a few hours of treatment and then became greater as a function of time (i.e., decreased superhydrophobicity). After 24 h of treatment at different temperatures (100, 150, and 200°C), all samples showed superhydrophobic property and exhibited the lotus and petal effects. Moreover, the Al, Cu, and Ti samples treated at 50°C showed superhydrophobic character with the petal effect

after a few days of heat treatment (six, two, and two days, respectively) (**Figure 6**). Additionally, the samples stored in ambient air without heat treatment showed relatively long wettability transition times before becoming superhydrophobic. While Cu became hydrophobic after 15 days (and had a CA that still increased over time), Al and Ti were still hydrophilic after 60 days. Therefore, adding a heat treatment process after laser ablation can reduce the wettability transition time from hydrophilic to superhydrophobic from several weeks/months to a few hours.

3.3. Continuous Heat Treatment

In our previous study,^[28] we found that water droplet contact from CA and SA measurement during heat treatment could affect the quality of superhydrophobic surface. Five samples for each heat treatment temperature (100, 150, and 200°C) were treated continuously for 6 h in an oven without any contact with water, as shown in **Figure 7**. At the highest temperature (200°C),

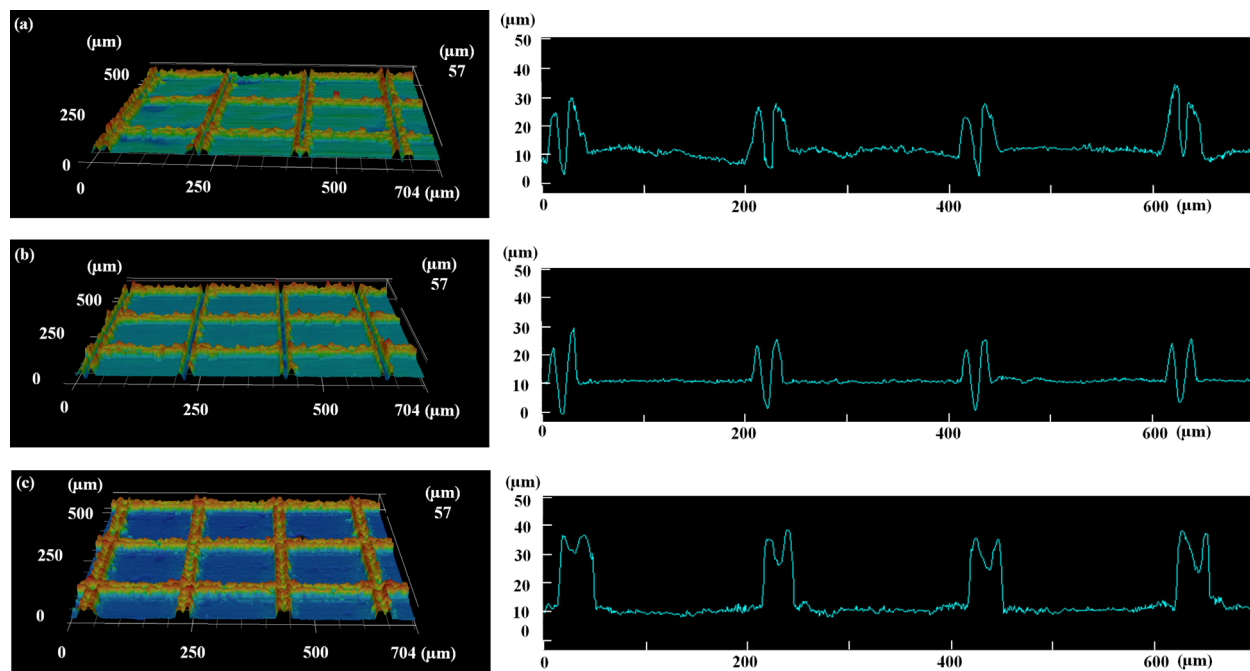


Figure 4. 3D confocal microscope images of laser-ablated a) Al, b) Cu, and c) Ti surfaces.

CAs and SAs of Al and Ti did not change much, and the samples were still superhydrophobic with lotus effect. Therefore, the effect of water might not be significant for Al and Ti samples treated at 200 °C. However, Cu samples treated at 200 °C showed clear change in SA. The Cu surfaces changed from petal effect (no SA) to lotus effect (SA < 10°). Therefore, water contact during heat treatment affected largely to Cu surface. The effect of water contact during heat treatment was confirmed clearly with increase in CAs of samples which were treated at 100 and 150 °C. Moreover, samples treated continuously at 150 °C for 6 h showed the appearance of the sliding angle. Additionally, the Al sample continuously treated for 6 h at 100 °C did not show any clear effects of water contact. This might come from an insufficient heat treatment time.

After continuous heat treatment for 6 h, samples were stored in ambient air, and their wettability was measured after 14 days and after 30 days in order to investigate the stability, as shown in Table 2. Samples treated continuously for 6 h at 200 °C showed stable superhydrophobicity; the contact angles were greater than

170° and the sliding angles were smaller than 10° for a long time (i.e., over one month). For the samples treated continuously for 6 h at 150 °C, the contact angles were also greater than 170°, but the sliding angles just after heat treatment were greater than 10° (except for Ti). However, after being stored in ambient air for a long period of time after heat treatment, the sliding angles of Al and Cu samples were improved and became smaller than 10°. The Al sample continuously treated for 6 h at 100 °C showed no clear improvement in wettability, while the Cu and Ti samples treated at these conditions showed hydrophobic character right after heat treatment. After being stored in ambient air for a long time, the contact angles of Cu and Ti increased, and the samples became superhydrophobic and showed the petal effect. Additionally, after 30 days, the Cu samples had large sliding angles. This could indicate that the samples treated continuously for 6 h at 100 or 150 °C can be improved continuously their wettability after heat treatment.

For practical applications and industrial processes, heat treatment at 200 °C for 6 h without any water contact might

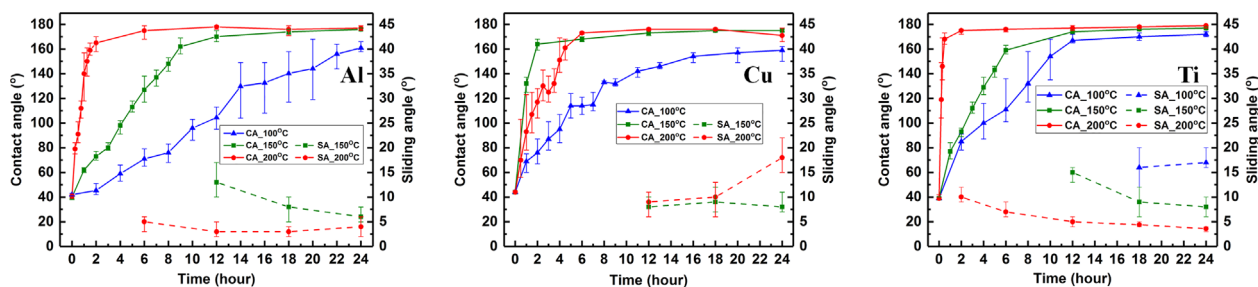


Figure 5. Contact angles and sliding angles of Al, Cu, and Ti samples measured at various times after heat treatment (100, 150, and 200 °C).

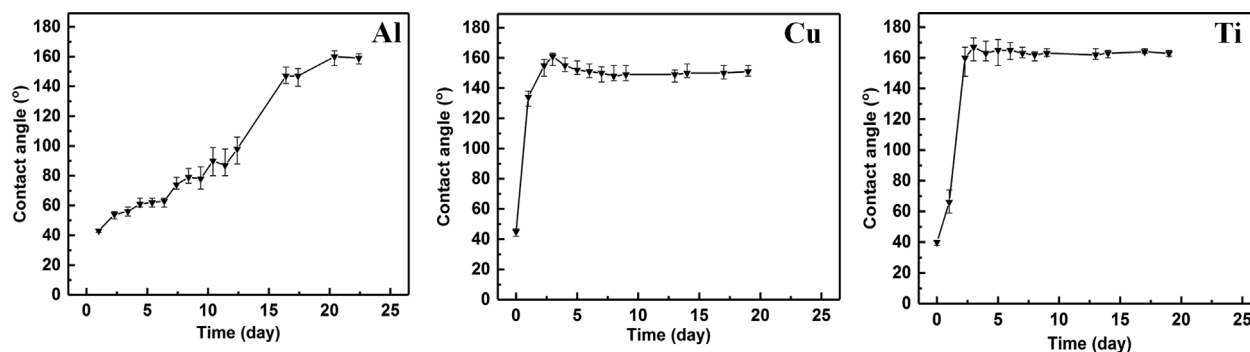


Figure 6. Contact angles of Al, Cu, and Ti samples measured at various times after heat treatment (50 °C).

represent good processing conditions. These conditions are appealing due to the sufficiently short heat treatment time combined with the high-quality superhydrophobicity and stability of the resultant material.

4. Discussion

4.1. Mechanism of the Wettability Transition

During pulsed laser ablation, the metallic surfaces showed metal oxide peaks, as shown in the XRD results in **Figure 8**. Oxidation processes occurred during laser fabrication. However, Al and Ti showed no difference in structures before and after heat treatment. Because the micro-burr structures on laser-ablated Al

and Ti did not change after heat treatment, the superhydrophobicity on Al and Ti surfaces might be caused by other factors. The EDS results indicated a clear increase in carbon content on the micro-burrs after the post-process heat treatment, as shown in **Table 3** and **4**. However, at the flat surfaces between ablated lines, no clear difference in the carbon content was observed after treatment.

We propose that organic adsorption onto the micro-burr structure occurred when laser-ablated Al and Ti samples were put in ambient air. The heat treatment process accelerated this organic adsorption. To confirm this mechanism, FT-IR measurements were carried out, as shown in **Figure 9**. After laser ablation, Al and Ti showed –OH functional groups on the micro-burrs. The presence of these groups on metal oxide films is known to lead to organic adsorption.^[29,30] Therefore, after laser

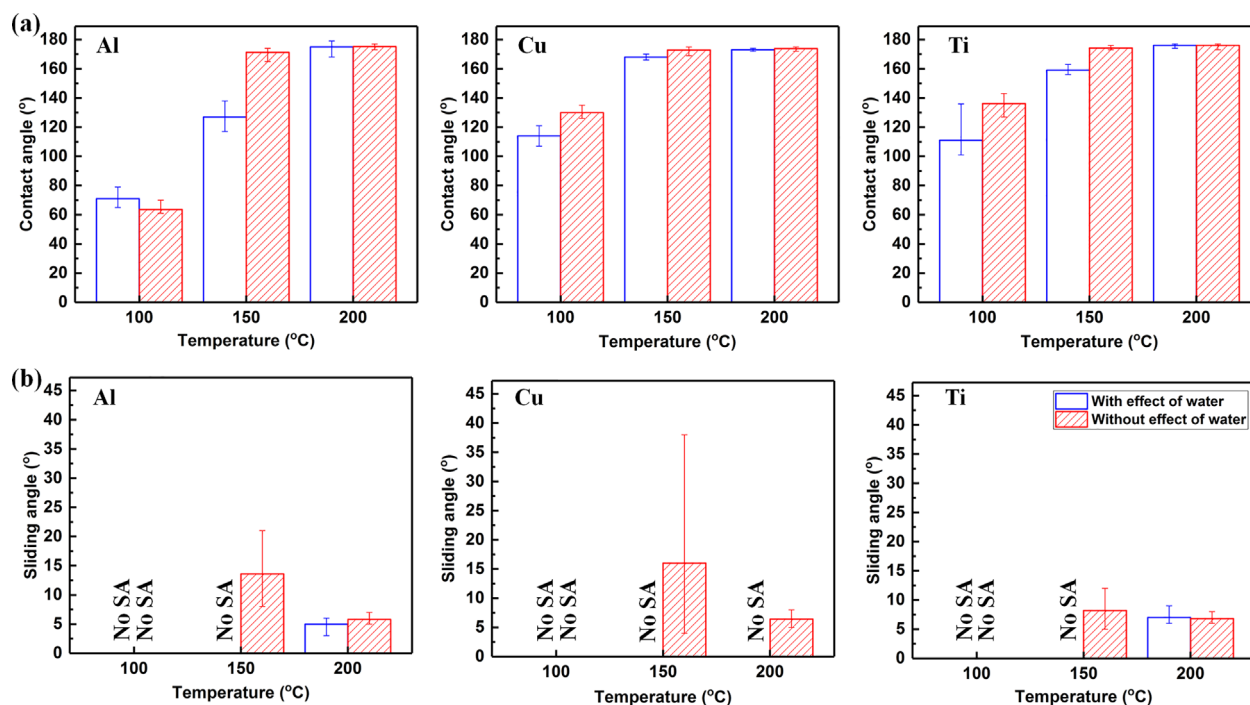


Figure 7. Effect of water during the wettability change of Al, Cu, and Ti samples: a) contact angles and b) sliding angles after 6 h of treatment.

Table 2. Wettability of laser-ablated Al, Cu, and Ti immediately (0 days), 14 days, and 30 days after the post-process heat treatment.

Material	Temperature (°C)	CA (°)			SA (°)		
		0 days	14 days	30 days	0 days	14 days	30 days
Al	100	64 ± 3.6	62 ± 5.5	62 ± 5.5	—	—	—
	150	171 ± 3.7	174 ± 1.6	174 ± 0.7	14 ± 5.0	6 ± 1.1	5 ± 1.3
	200	175 ± 1.5	176 ± 0.9	175 ± 1.1	6 ± 0.8	5 ± 1.6	5 ± 1.2
Cu	100	130 ± 3.2	160 ± 1.3	162 ± 2.5	—	—	43 ± 9.3
	150	173 ± 2.4	174 ± 0.9	174 ± 1.3	16 ± 13.3	9 ± 3.1	9 ± 2.9
	200	174 ± 1.1	174 ± 0.9	174 ± 1.5	6 ± 1.5	7 ± 1.7	7 ± 2.4
Ti	100	136 ± 5.8	166 ± 3.4	166 ± 7.9	—	—	—
	150	174 ± 1.1	176 ± 1.1	175 ± 1.1	8 ± 3.5	8 ± 1.9	8 ± 1.5
	200	176 ± 1.7	176 ± 1.1	175 ± 1.1	6.8 ± 0.8	7 ± 0.4	7 ± 1.1

ablation, metal oxides with OH groups can adsorb organic matter from ambient air, causing several weak hydrophobic groups ($-\text{CH}_3$, $\text{C}=\text{C}$, or $\text{C}=\text{O}$) to appear on the burrs. Using the heat treatment, the organic adsorption process was accelerated, and strong hydrophobic groups ($-\text{CH}_3$ and $-\text{CH}_2$) appeared on the heat-treated Al and Ti micro-burrs. At the same time, the $-\text{OH}$ groups were disappeared after heat treatment. The unchanging crystalline structures, increased carbon content, and appearance of strong hydrophobic groups demonstrated that organic adsorption was occurred on the laser-ablated Al and Ti micro-burrs. The organic matter can produce a hydrophobic layer on the rough micro-burr structures, and results in superhydrophobicity in Al and Ti surfaces. This mechanism on Al and Ti is in good agreement with the findings of other studies. The organic adsorption or accumulation of carbon was found on laser-ablated Al that was stored in ambient air for a long time,^[31,32] and the adsorption of organics was also observed on aluminum oxide.^[33–36] CO_2 decomposition, which is a type of organic adsorption, was also found on laser-ablated Ti that was stored in ambient air for a long time.^[22,37,38]

In our previous research,^[27] the mechanism for copper to change from hydrophilicity to superhydrophobicity was the reduction of CuO to Cu_2O . The EDS results in that study showed an increase in Cu concentration on the micro-burrs after heat treatment, which supports this mechanism. In the present

research, the copper content on the micro-burrs after heat treatment also increased, as shown in **Table 5**. Additionally, two new Cu_2O peaks were observed in the XRD results; these appeared after heat treatment and support the reduction-based mechanism, as shown in Figure 8. The FT-IR results for copper before heat treatment showed the presence of $-\text{OH}$ groups, similar to the cases of Al and Ti, as shown in Figure 9. These groups can adsorb organic matter in ambient air; therefore, a small peak related to $-\text{CH}_3$ groups appeared in the results of the treated sample. However, there was no clear difference in the FT-IR results before and after heat treatment. Therefore, organic adsorption might not be important factor for the wettability transition mechanism. After heat treatment, which led to an increase in copper content and the appearance of Cu_2O peaks, the mechanism behind the wettability transition in copper was driven by the change in the crystalline structure as CuO was reduced to Cu_2O . Hydrophobic Cu_2O with rough micro-burr structures caused the surface to become superhydrophobic.

4.2. Potential Applications

The quality of superhydrophobic Al, Cu, and Ti surfaces was demonstrated by analyzing the contact of water droplets and the bouncing effect. For this, 7 μL water droplets were placed onto

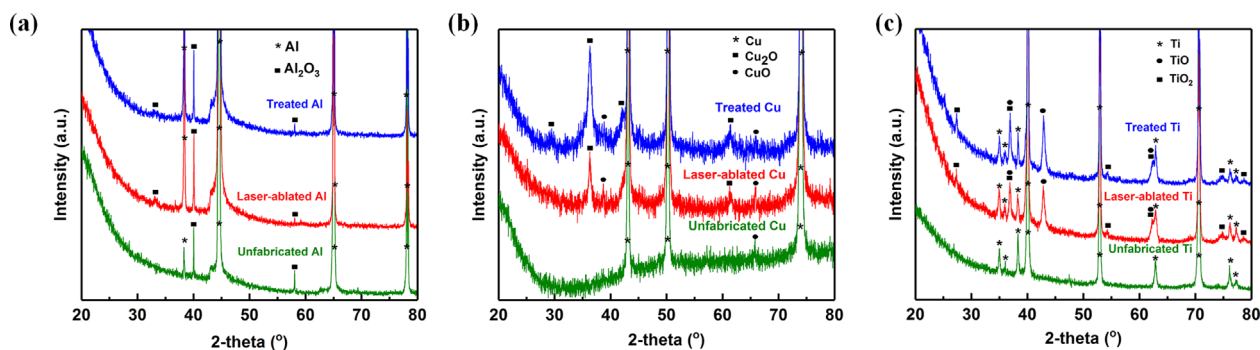


Figure 8. XRD results of unprocessed, laser-ablated, and treated Al, Cu, and Ti surfaces.

Table 3. Chemical composition on Al burrs right after laser ablation and on heat-treated Al burrs.

Element	Burr just after laser ablation			Heat-treated burr (6 h)		
	Ave	Err+	Err-	Ave	Err+	Err-
C	1.50	0.77	1.50	13.64	1.40	0.86
O	67.51	0.66	0.92	59.37	0.59	0.88
Al	30.99	0.84	0.99	27.00	1.43	2.00
O/Al	2.18	—	—	2.20	—	—
C/Al	0.05	—	—	0.51	—	—

Table 4. Chemical composition on Ti burrs right after laser ablation and on heat-treated Ti burrs.

Element	Burr just after laser ablation			Heat-treated burr (6 h)		
	Ave	Err+	Err-	Ave	Err+	Err-
C	3.37	0.70	0.82	10.82	0.12	0.10
O	75.95	2.17	1.34	70.18	2.10	1.72
Ti	20.68	2.16	2.28	19.00	1.81	2.22
O/Ti	3.67	—	—	3.69	—	—
C/Ti	0.16	—	—	0.57	—	—

Table 5. Chemical composition on Cu burrs right after laser ablation and on heat-treated Cu burrs.

Element	Burr on fresh			Burr on treat (6 h)		
	Ave	Err+	Err-	Ave	Err+	Err-
O	52.83	2.57	3.26	28.60	7.83	5.92
Cu	47.17	3.26	2.57	71.40	5.92	7.83
O/Cu	1.12	—	—	0.40	—	—

the Al, Cu, and Ti micro-burr structures, as shown in **Figure 10** and in Video S1. The water droplets were compressed or even slid off the needle, but they still could not be separated from the needle to be placed on the surfaces; droplets also showed

vibrations after moving up the needle from the surfaces. Additionally, 10 μ L water droplets were dropped from a height of 5 cm onto Al, Cu, and Ti surfaces tilted at 8°, as shown in **Figure 11** and in Video S2. These water droplets bounced off the surfaces. The good performance of the superhydrophobic surface was also demonstrated by the bouncing of many continuously-dropped water droplets on the surfaces. The high-quality superhydrophobicity obtained on surfaces treated by laser ablation with a post-process heat treatment can be used for self-cleaning applications, as shown in **Figure 12** and in Video S3. The water droplets easily removed white powder from the surfaces tilted at 8°.

Due to the short fabrication time and the fact that no harsh chemicals were used, these superhydrophobic Al, Cu, and Ti surfaces could be applied in a variety of potential applications such as water positioning/water storage and liquid transport/control of water adhesion. By designing proper patterns on metallic surfaces, as shown **Figure 13** and Video S4 with Ti, water droplets can be stored or positioned on unfabricated areas with desired shapes and volumes; these droplets could be then utilized for bio-applications. By controlling the treatment time and/or treatment temperature, the sliding angles can be controlled. Therefore, water adhesion on these surfaces is different and has the potential to be used for liquid transport.^[18,39]

5. Conclusion

Without using any chemicals, superhydrophobic laser-ablated metallic surfaces can be fabricated in a short period of time by employing a facile post-process heat treatment. The effect of different heat treatment temperatures was studied. With increasing heating temperature, the wettability transition time could be reduced for Al and Ti. However, a higher temperature (200 °C) might decrease the quality of Cu superhydrophobic surfaces. Compared to samples aged for a long time, the samples made with the proposed post-process heat treatment after laser ablation could reduce the wettability transition time from several weeks/months to several hours (or even less than 6 to 1 h when using a temperature of 200 °C). The effect of water droplet contact during heat treatment at different temperatures was also investigated. The mechanism of the wettability change was determined to be driven by a combination of surface chemistry

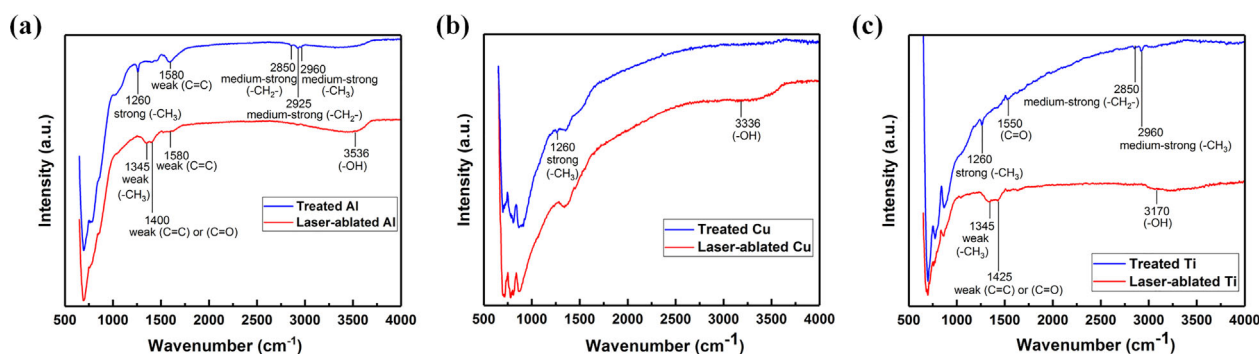


Figure 9. FT-IR results of laser-ablated and treated Al, Cu, and Ti surfaces.

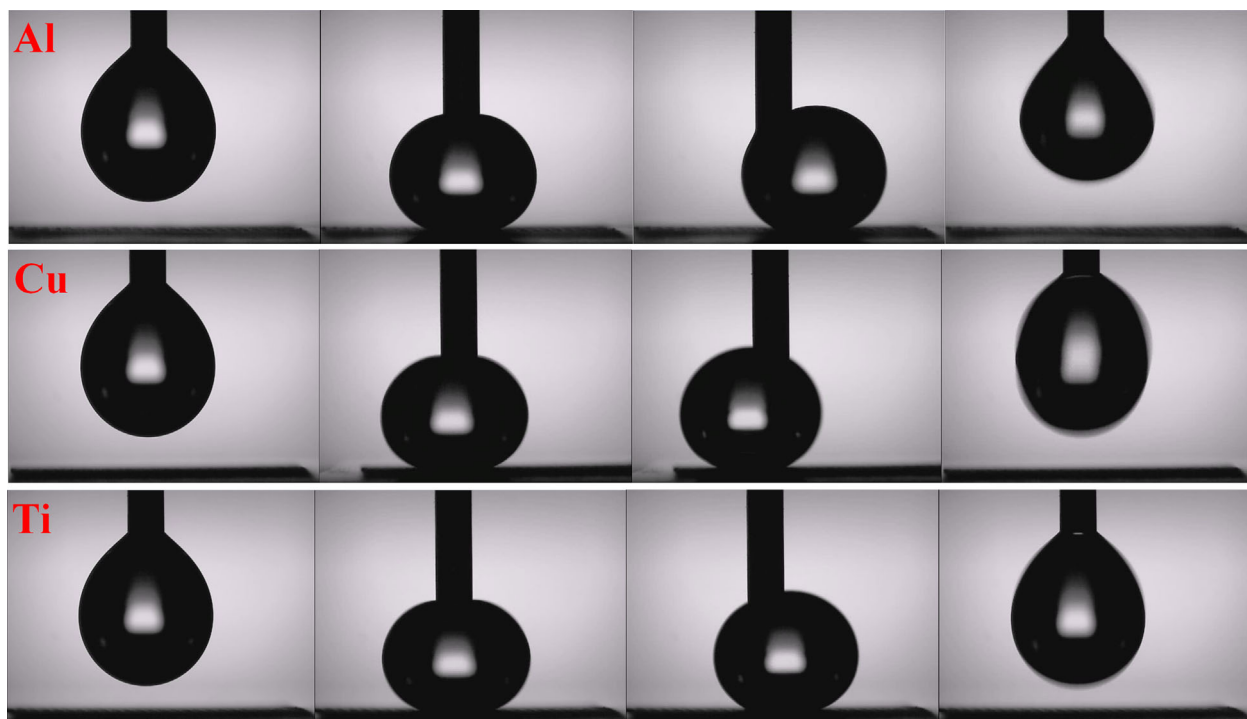


Figure 10. Placement of 7 μL water droplets onto Al, Cu, and Ti micro-burr structures.

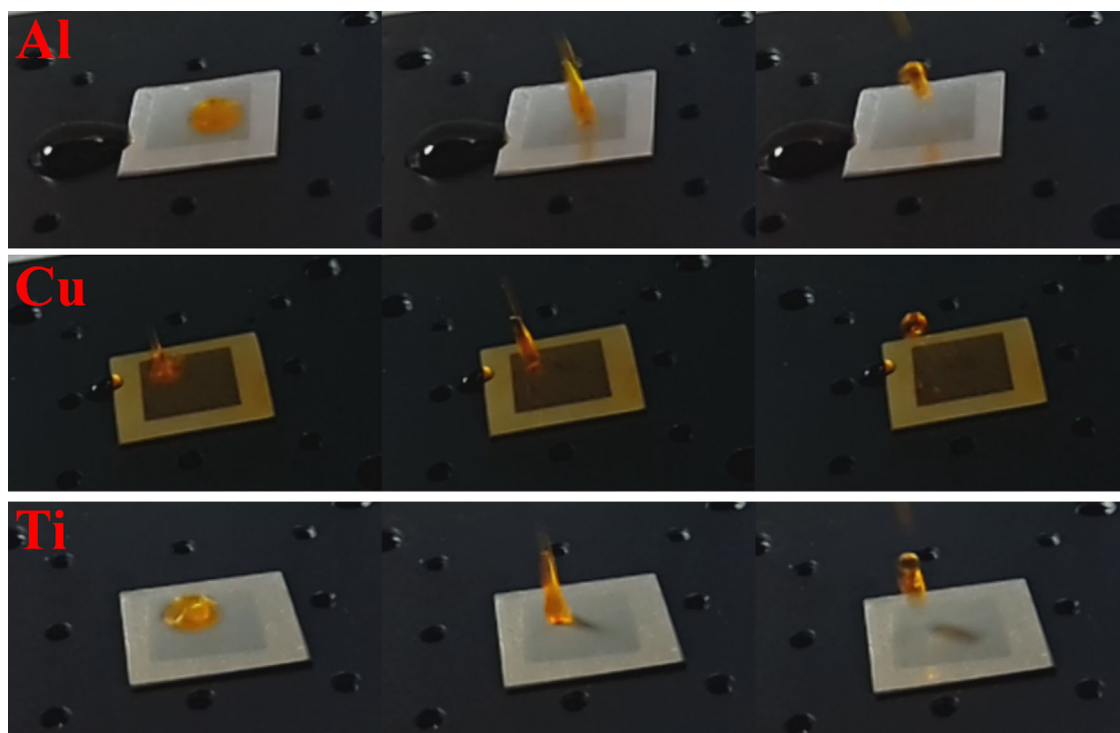


Figure 11. Bouncing of 10 μL water droplets dropped from an initial height of 5 cm on Al, Cu, and Ti superhydrophobic surfaces.

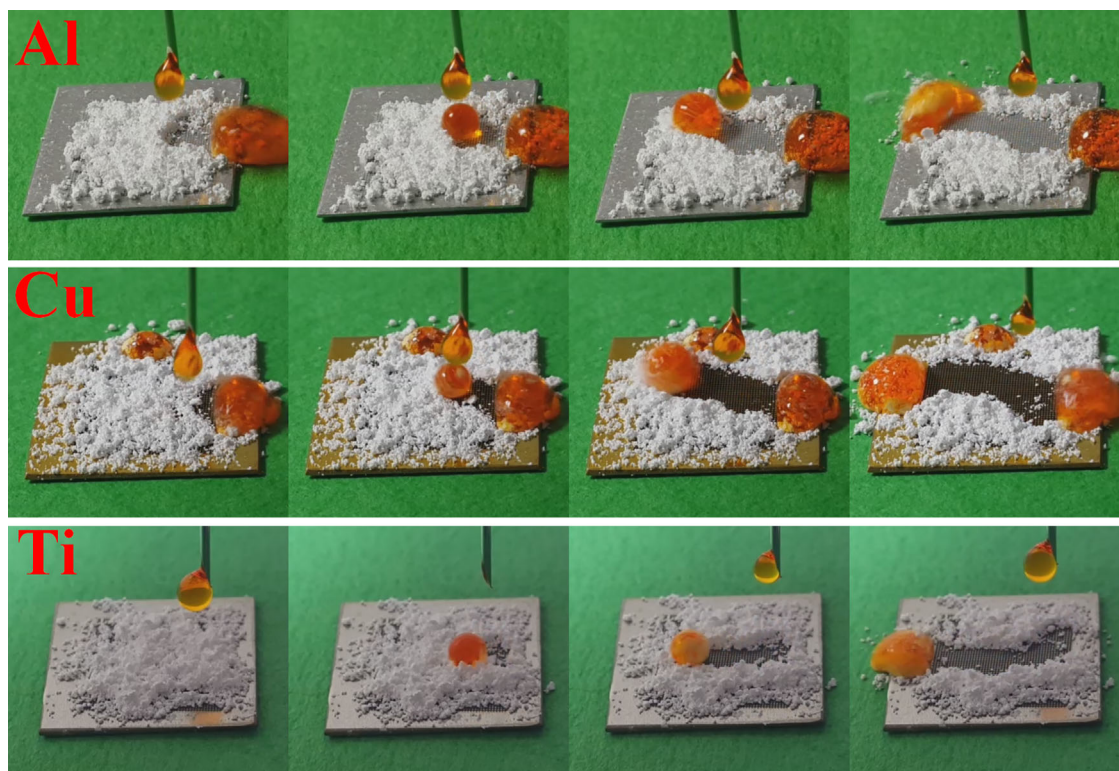


Figure 12. Self-cleaning procedure during which sliding water droplets carry away white powder on Al, Cu, and Ti superhydrophobic surfaces.

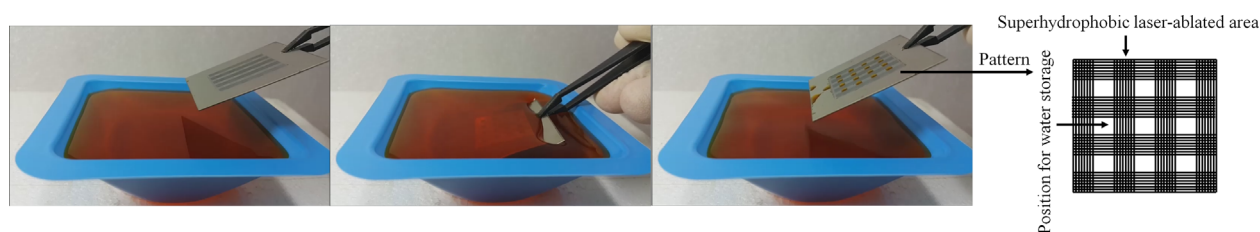


Figure 13. Water positioning on a Ti superhydrophobic patterned surface.

through organic adsorption and micro-burr structure for Al and Ti. Alternatively, it was driven by a change in the material's crystalline structure on micro-burrs through the reduction of CuO to Cu₂O for Cu. The high performance of these superhydrophobic metallic surfaces was also demonstrated. Additionally, several potential applications, such as self-cleaning, water positioning, and water transport, were proposed.

Acknowledgements

This work was supported by a National Research Foundation of Korea (NRF) grant (No. NRF-2018R1A2B6004012).

Conflict of Interest

The authors declare no conflict of interest.

Supporting Information

Supporting Information is available online from Wiley Online Library or from the author.

Keywords

Heat Treatment, Nanosecond Laser Ablation, Self-Cleaning, Superhydrophobic Metallic Surface, Water Positioning

Received: December 5, 2017
Revised: February 1, 2018
Published online: March 14, 2018

[1] E. J. Cheng, J. Sakamoto, J. Salvador, H. Wang, R. Maloney, T. Thompson, *Acta Mater.* **2017**, 127, 450.

- [2] C.-V. Ngo, G. Davaasuren, H.-S. Oh, D.-M. Chun, *Int. J. Precis. Eng. Manuf.* **2015**, 16, 1347.
- [3] D.-M. Chun, G. Davaasuren, C.-V. Ngo, C.-S. Kim, G.-Y. Lee, S.-H. Ahn, *CIRP Ann. – Manuf. Technol.* **2014**, 63, 525.
- [4] A. Pakdel, X. Wang, Y. Bando, D. Golberg, *Acta Mater.* **2013**, 61, 1266.
- [5] G. Davaasuren, C.-V. Ngo, H.-S. Oh, D.-M. Chun, *Appl. Surf. Sci.* **2014**, 314, 530.
- [6] R.-C. Wang, C.-Y. Chao, W.-S. Su, *Acta Mater.* **2012**, 60, 2097.
- [7] C.-V. Ngo, D.-M. Chun, *Sci. Rep.* **2016**, 6, 36735.
- [8] Y. He, Y. Wu, J. Fu, Q. Gao, J. Qiu, *Electroanalysis* **2016**, 28, 1658.
- [9] A. Lozhechnikova, H. Bellanger, B. Michen, I. Burgert, M. Österberg, *Appl. Surf. Sci.* **2017**, 396, 1273.
- [10] J. E. Mates, R. Ibrahim, A. Vera, S. Guggenheim, J. Qin, D. Calewatts, D. E. Walldrop, C. M. Megaridis, *Green Chem.* **2016**, 18, 2185.
- [11] V. H. Tran Thi, B.-K. Lee, C.-V. Ngo, *J. Taiwan Inst. Chem. Eng.* **2017**, 71, 527.
- [12] K. Seo, M. Kim, D. H. Kim, *Carbon N. Y.* **2014**, 68, 583.
- [13] B. Zheng, G. Jiang, W. Wang, X. Mei, *Radiat. Eff. Defects Solids* **2016**, 171, 461.
- [14] K. M. Tanvir Ahmmed, A.-M. Kietzig, *Soft Matter* **2016**, 12, 4912.
- [15] S. Pan, N. Wang, D. Xiong, Y. Deng, Y. Shi, *Appl. Surf. Sci.* **2016**, 389, 547.
- [16] Z. Zhang, B. Ge, X. Men, Y. Li, *Colloids Surf. A Physicochem. Eng. Aspects* **2016**, 490, 182.
- [17] H. Zhu, Z. Guo, W. Liu, *Chem. Commun.* **2016**, 52, 3863.
- [18] T. Chen, H. Liu, S. Teng, W. Yan, H. Yang, J. Li, *J. Vac. Sci. Technol. A Vacuum, Surf., Film* **2016**, 34, 61103.
- [19] D. V. Ta, A. Dunn, T. J. Wasley, R. W. Kay, J. Stringer, P. J. Smith, C. Connaughton, J. D. Shephard, *Appl. Surf. Sci.* **2015**, 357, 248.
- [20] M. Tang, V. Shim, Z. Y. Pan, Y. S. Choo, M. H. Hong, *J. Laser Micro/Nanoeng.* **2011**, 6, 6.
- [21] R. Jagdheesh, J. J. García-Ballesteros, J. L. Ocaña, *Appl. Surf. Sci.* **2016**, 374, 2.
- [22] C. Yang, X. Mei, Y. Tian, D. Zhang, Y. Li, X. Liu, *Int. J. Adv. Manuf. Technol.* **2016**, 87, 1663.
- [23] D. H. Kam, S. Bhattacharya, J. Mazumder, *J. Micromech. Microeng.* **2012**, 22, 105019.
- [24] B. Li, H. Li, L. Huang, N. Ren, X. Kong, *Appl. Surf. Sci.* **2016**, 389, 585.
- [25] P. N. Saltuganov, A. A. Ionin, S. I. Kudryashov, A. A. Rukhadze, A. I. Gavrilov, S. V. Makarov, A. A. Rudenko, D. A. Zayarny, *J. Russ. Laser Res.* **2015**, 36, 81.
- [26] S. Moradi, S. Kamal, P. Englezos, S. G. Hatzikiriakos, *Nanotechnology* **2013**, 24, 415302.
- [27] D.-M. Chun, C.-V. Ngo, K.-M. Lee, *CIRP Ann. – Manuf. Technol.* **2016**, 65, 519.
- [28] C.-V. Ngo, D.-M. Chun, *Appl. Surf. Sci.* **2017**, 409, 232.
- [29] S. Takeda, M. Fukawa, Y. Hayashi, K. Matsumoto, *Thin Solid Films* **1999**, 339, 220.
- [30] B. Gu, J. Schmitt, Z. Chen, L. Liang, J. F. McCarthy, *Geochim. Cosmochim. Acta* **1995**, 59, 219.
- [31] J. Long, M. Zhong, H. Zhang, P. Fan, *J. Colloid Interface Sci.* **2015**, 441, 1.
- [32] P. Bizi-Bandoki, S. Valette, E. Audouard, *Appl. Surf. Sci.* **2013**, 273, 399.
- [33] J. Van den Brand, S. Van Gils, P. C. J. Beentjes, H. Terryn, J. H. W. De Wit, *Appl. Surf. Sci.* **2004**, 235, 465.
- [34] J. Van den Brand, O. Blajiev, P. C. J. Beentjes, H. Terryn, J. H. W. De Wit, *Langmuir* **2004**, 20, 6308.
- [35] J. Van den Brand, O. Blajiev, P. C. J. Beentjes, H. Terryn, J. H. W. De Wit, *Langmuir* **2004**, 20, 6318.
- [36] Ö. Özkanat, B. Salgin, M. Rohwerder, J. M. C. Mol, J. H. W. de Wit, H. Terryn, *J. Phys. Chem. C* **2012**, 116, 1805.
- [37] A.-M. Kietzig, S. G. Hatzikiriakos, P. Englezos, *Langmuir* **2009**, 25, 4821.
- [38] S. Moradi, N. Hadjesfandiari, S. Toosi, *ACS Appl. Mater. Interfaces* **2016**, 8, 17631.
- [39] C.-F. Wang, T.-W. Hsueh, *J. Phys. Chem. C* **2014**, 118, 12399.